Published by IOP Publishing for Sissa Medialab

Received: *October 31, 2019*
Accepted: *December 20, 2019*
Published: *January 31, 2020*

TECHNICAL REPORT

High-bandwidth magnet power supply for iron core corrector in Taiwan Photon Source

J.-C. Huang,[1] Y.-S. Wong,[2] K.-B. Liu, C.-Y. Liu, B.-S. Wang and Y.-L. Chu

National Synchrotron Radiation Research Center,
101, Hsin-Ann Rd., Hsinchu 300, Taiwan

E-mail: wong.ys@nsrrc.org.tw

Abstract: Taiwan Photon Source (TPS) has been operated for 6 years, and the mean time between fails has reached world-class standards since the first light was delivered on 31 December 2013. To maintain satisfactory research facilities, all subsystems are constantly updating their equipment. The power supply group dramatically increases the output current bandwidth on bipolar corrector magnet power supplies, thereby increasing the number of calculations of the fast orbit feedback system and improving the stability of beam current. Finally, a DC/DC high-bandwidth corrector was built in the laboratory with the maximum prototype output current and voltage of 10 A/40 V. The power switch is metal-oxide-semiconductor field-effect transistor (MOSFET,) and the power state is a full-bridge (H-Bridge) circuit with a 145 kHz signal. The effectiveness of the control loop design can be verified from the gain margin and output current ripple. The prototype achieved a 11 kHz bandwidth with less than 3 dB attenuation for a reference signal of 0.1 V (equal to 0.1 A). Finally, a hardware prototype circuit was constructed in a power group laboratory. It had an input voltage of 48 V, output current of 10 A and maximum power of 400 W.

Keywords: Accelerator Subsystems and Technologies; Hardware and accelerator control systems; Accelerator Applications; Instrumentation for particle accelerators and storage rings - low energy (linear accelerators, cyclotrons, electrostatic accelerators)

[1]First author.
[2]Corresponding author.

https://doi.org/10.1088/1748-0221/15/01/T01005

2020 JINST 15 T01005

Contents

1 Introduction

Light is made up of electromagnetic waves and is an important basis for human beings to observe nature. In addition to visible light, electromagnetic waves also comprise radio waves, microwaves, infrared light, ultraviolet light, X-rays and gamma rays depending on the wavelength. Different light sources play varying functions in human history because of their characteristics. "Synchronous accelerator light source" covers electromagnetic waves in the wavelength range of infrared light, visible light, ultraviolet light and X-ray. It was first discovered in 1947 on the synchrotron of General Electric Company of the United States. Light's continuous wavelength, extremely high brightness, small cross-sectional area and wavelength range that covers tens of microns to several hundredths of a nanometres can help scientists observe the world that is invisible to the naked eye. The synchrotron source illuminates the material and produces different effects, such as photoelectron emission, ion or neutral atom detachment, absorption, scattering and diffraction. Each effect is closely related to the physical or chemical properties of the substance itself [1, 2]. Therefore, the use of synchrotron light source to observe the substance accurately allows the exploration of the internal structure of the substance and the interaction among the electrons within. In the 21st century, synchrotron light sources have become cutting-edge basic scientific research materials that can be widely used in materials, biology, medicine, physics, chemistry, chemical, geology, archaeology, environmental protection, energy, electronics and micro-mechanics [3]–[5].

The modified magnet power supply has a full-scale modular design. It consists of a control module and eight power modules. The control signals are provided by the control module and distributed to the power modules via the backplane. When each monitoring signal shows an

2020 JINST 15 T01005

abnormality, the interlock mechanism starts to turn off the output current until the reset signal is released. The chassis specifications are in accordance with the IEC standard 19-inch standard chassis, and the motherboard and module circuit board dimensions and connectors follow relevant IEC specifications. The heat dissipation of the chassis is obtained by the fan below and blown out by the fan above. The front panel is equipped with LED lights to indicate system status. For the corrector power supply specification, the input voltage is 48 V, and the output current and voltage are ±10 A and ±40 V, respectively. In this study, the output loading is an iron core with an inductance of 1 mH. A 0.1-Ω resistor was used. Iron is the cheapest material, its core loss is higher than that of more advanced alloys, but this property can be compensated by increasing the core size. This material is advantageous in situations where cost is more important than mass and size. Saturation flux was set to approximately 1 to 1.5 Tesla. Relatively high hysteresis and eddy current loss were observed, and operation was limited to low frequencies (approximately below 100 kHz). The following are used in energy storage inductors: DC output chokes, differential mode chokes, chokes for power factor[1] correction, resonant inductors and pulse and Flyback transformers [6]–[9].[2] The binder used is usually epoxy or other organic resins that are susceptible to thermal aging. At temperatures higher than 125°C, the binder is degraded, and the core magnetic properties may change. By using heat-resistant binders, the cores can be used up to 200°C.

Fast orbit feedback (FOFB) system requires a current ripple of less than ±0.1 mA peak-to-peak at 1–5 kHz. In addition, the current setting resolution is 20 bits, whereas the current feedback resolution is 19 bits at full scale 10 A. Hence, the maximum resolution reaches 64 µA. Therefore, this paper designed a high-resolution, high feedback system and low-output ripple DC–DC corrector power supply to supply energy to a corrector iron magnet [10]–[14]. This power supply can verify the output current ripple under 50 µA at a full load of 10 A output current. The bandwidth can achieve over 5 kHz. The national synchrotron light source FOFB can increase the detection from 200 times/second to 5,000 times/second. The stability of beam current can be greatly improved.

2 Correction power supply, power stage and auxiliary power stage

2.1 Power stage

This traditional full bridge circuit is selected as corrector power supply that can easily change the polarity of an output current to a load. The power stage includes an input filter, full bridge circuit and output filter. The input filter is for the electromagnetic interference (EMI) and noise. It comprises a 10 µH parallel inductor filter and a 470 µF/100 V capacitor filter (4 pcs). Full bridge was combined with four MOSFET IXFK180N15 with voltage and current rating of 150 V and 180 A, respectively, and $R_{ds(\mathrm{on})}$ =11 mΩ. The output filter is a 60 µH parallel output inductor filter (2 pcs) and 0.82 µF/100 V output filter capacitor (6 pcs) with damping components. The power state circuit structure is shown in figure 1. An H-bridge is an electronic circuit that switches the polarity of a current applied to a load. The output loading has positive current when S_1 and S_4 are turned on, and S_2 and S_3 are turned off. The input power supplies energy to the output load depending on the duty cycle. Alternately, output loading has a negative current when S_2 and S_3 are turned on,

[1]https://en.wikipedia.org/wiki/Power_factor.

[2]https://en.wikipedia.org/wiki/Magnetic_core#cite_note-coilws-4.

and S_1 and S_4 are turned off. S_1, S_3, S_2 and S_4 cannot be turned on at the same time, because short circuit may occur and damage the component.

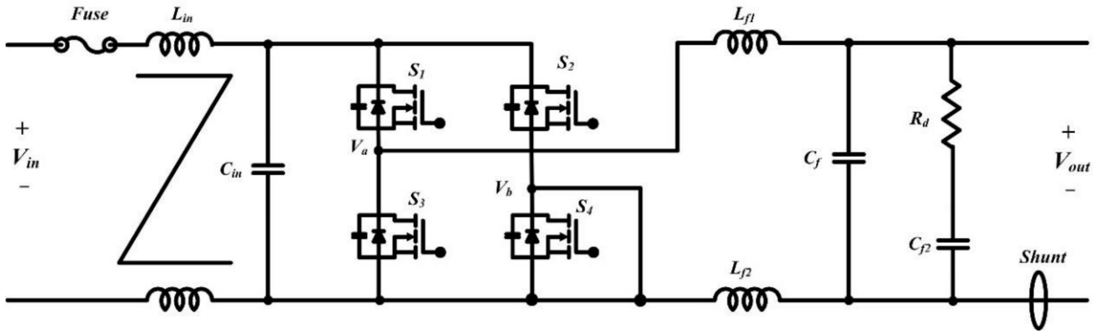

Figure 1. H-bridge circuit structure.

The output shunt used was the RUG-Z-R-100-0.1-TK1 product by ISABELLEN Ltd., which is a high-resolution current feedback sense. It was used to measure the current and provide the feedback signal for the current regulation. It has a resistor value of 100 mΩ, tolerance of 0.1%, temperature coefficient of <1 ppm/k and load capacity of 250 W. Figure 2 shows the shunt resistor component.

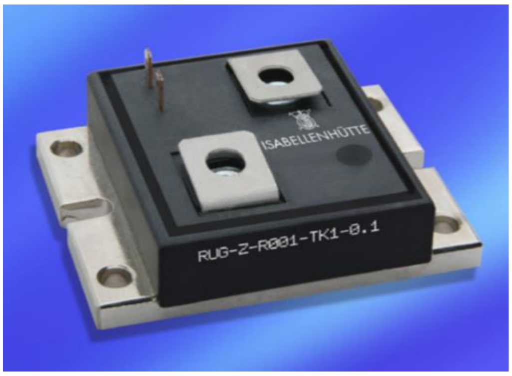

Figure 2. Shunt resistor RUG-Z-R001-TK1-0.1.

2.2 Auxiliary power

Auxiliary power refers to the electric power provided by an alternate source that serves as backup for the primary power source at the station main bus or prescribed sub-bus. This high bandwidth power supply uses a regulator integrated circuit (IC) to provide high stability DC voltages of approximately +15 V, +5 V, −15 V, +12 V, +8 V and −8 V supplied to the control IC or operation amplifier. A voltage regulator is an IC that provides a constant fixed output voltage regardless of the change in the load or input voltage. IC 78L08 has an input voltage of +15 V and an output voltage that supplies +8 V. IC 79L08 has an input voltage of −15 V and output voltage of −8 V. IC 7812 has an input voltage of +15 V and output voltage of +12 V. Figure 3 shows the auxiliary power circuit in this prototype.

2020 JINST 15 T01005

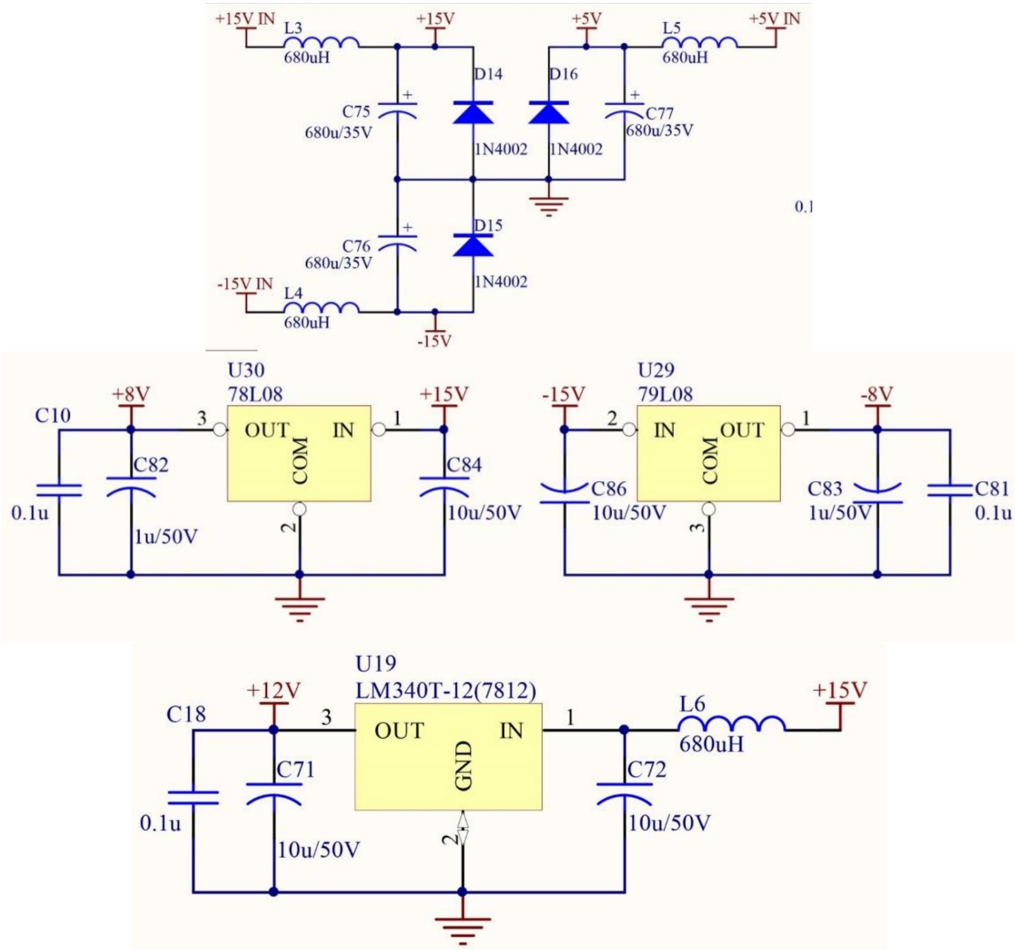

Figure 3. Auxiliary power circuit.

3 Corrector power supply protection circuit and control circuit

3.1 Protection circuit

The protection circuit is an important part of power electronics. It is related to safe and stable operation issues in the power electronics. This power supply is equipped with damping load temperature protection (T-R36 & T-R37), heat sink temperature protection (T-Heat Sink), pulse width modulation (PWM) power protection (PWM POWER), high voltage protection (HV POWER) and current over loading protection (IOVL). Upon receiving the fault signal, the power supply immediately stops supplying power. Figure 4 shows the protection circuit of the corrector magnet power supply.

(1) T-R36, T-R37, T-Heat Sink: damping load and heat sink temperature protection occur when the damping resistor and heat sink temperatures exceed 70°C, and the TMP01 output signal shifts from low to high levels.

(2) PWM Power: the UC3525 of pulse width modulator integrated circuits are designed to offer improved performance and decreased external part count when used to design all types of

switching power supplies. This IC failure leads to a disorder in the switch timing, thereby resulting in short circuit. Hence, UC3525 pulse width modulator integrated circuits fault triggers the signal of the PWM power.

(3) HV Power: most electronic converters include an under-voltage lockout (UVLO) function to disable the converter. Subsequently, the input power source is left with low voltage and protects the device from damage. When the supply voltage is very low and has no relevant protection, the function and performance of the converter may be undefined. For example, the logic circuit could malfunction or the MOSFET may operate in the linear region mode instead of the saturation mode, thereby releasing a large amount of heat in the MOSFET and eventually causing damage. For this prototype, the normal operation voltage is 48 V, and the HV power fault signal is triggered at an input voltage of less than 45 V.

(4) IOVL: overload protection provides prevents the existence of a running overcurrent that would cause overheating of the protected equipment. This prototype has a maximum output current rating of ±10 A and ±40 V. Therefore, when the system has over ±10 A or ±40 V, IOVL fault signal occurs, and the energy supply stops.

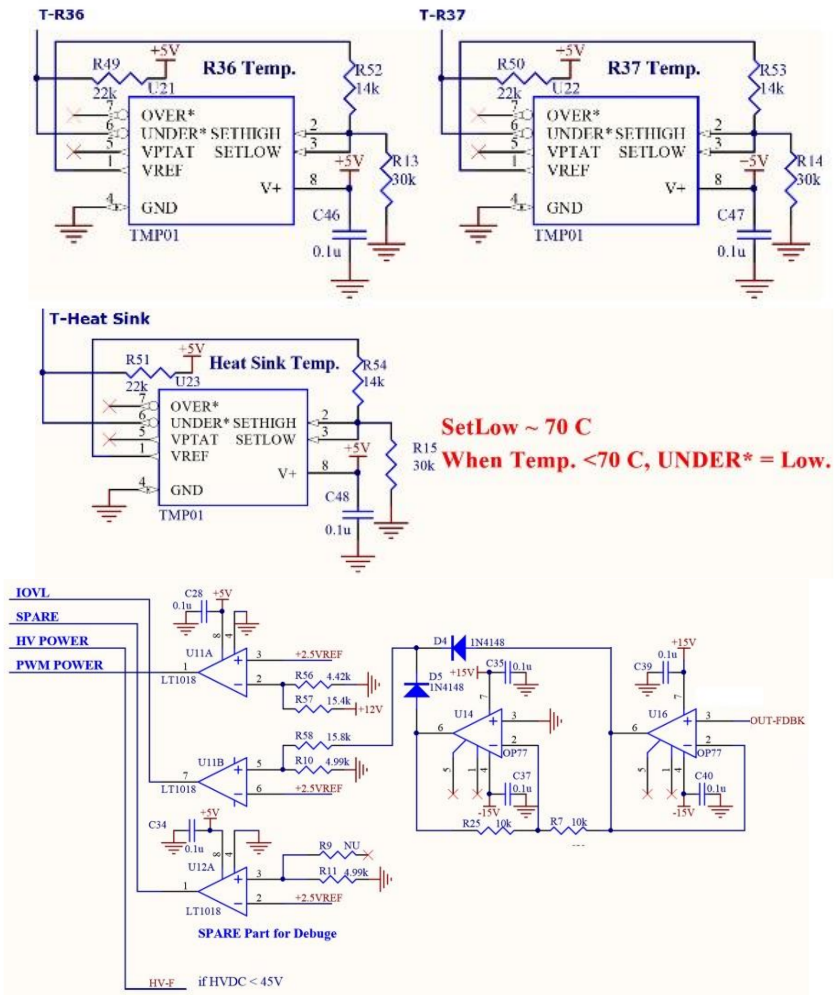

Figure 4. Protection circuit.

2020 JINST 15 T01005

3.2 Control circuit and MOSFET driver circuit

A closed loop control system is a set of electronic devices that automatically regulates a process variable to a desired state or set point without human interaction. The closed loop has a proportional integral (PI) controller, which is a feedback control loop that calculates an error signal by taking the difference between the outputs of a system. The input signals of the PI controller are the reference and feedback signals. The reference signal is the high-precision signal source provided by the user. The central control board is set to 1 V reference signal corresponding to the 1 A output current. The feedback signal is generated by the voltage converted from the current flowing through the shunt resistor. The second-order control of the PI controller is composed of resistors and capacitors. Changing the parameters of the components adjusts the gain margin and phase margin of the converter. This condition is critical for correcting the bandwidth and stability of the converter. The output signal of the PI controller is provided to the UC3525 for comparison with the built-in oscillator frequency. For this control circuit, the oscillator frequency is designed at 145 kHz. After operating the UC3525 pulse width modulation integrated circuit, a high-frequency PWM signal is generated, and the power component MOSFET IXFK 180N15 is driven by the HIP4081 driver IC. Figure 5 shows the power converter feedback voltage system, which comprises a PI controller circuit, pulse width modulation circuit and MOSFET drive circuit.

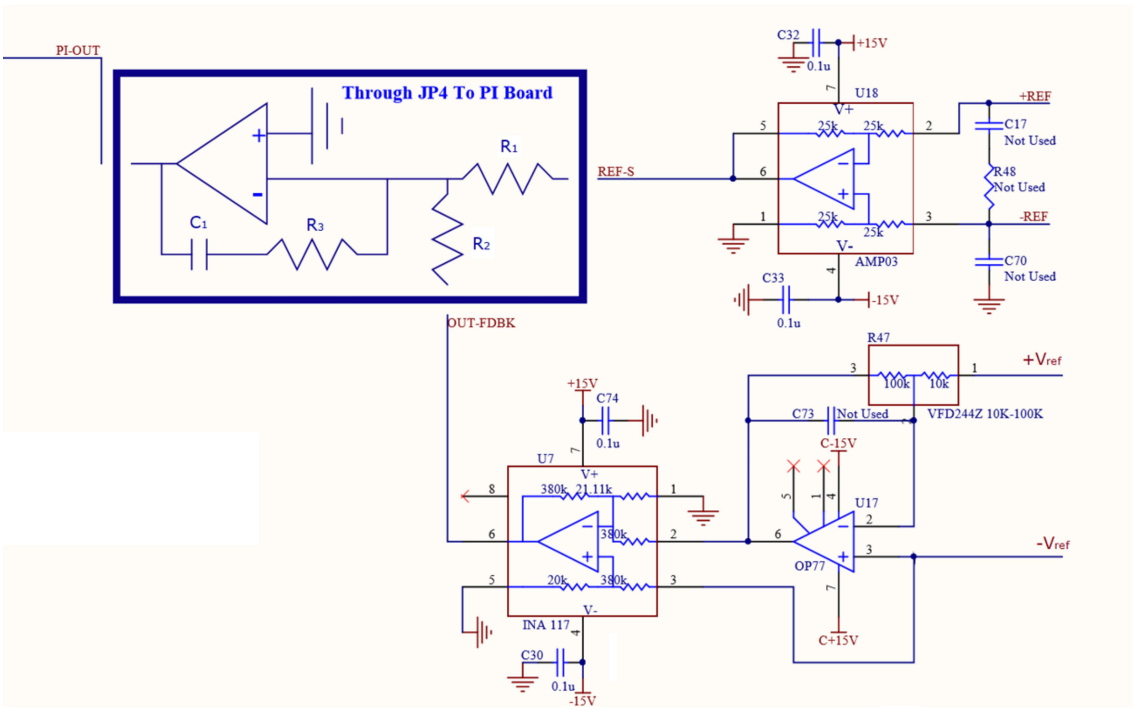

Figure 5. Control circuit and MOSFET driver circuit.

4 Experimental result of the output current ripple, bandwidth and current stability

For this study, the prototype fast corrector power supply was tested using a horizontal 15 mH corrector and 98 mΩ iron magnet by the National Synchrotron Radiation Research Center (NSRRC), which is normally field 116 Gauss and bending angle 35.8 µrad. Iron is the cheapest material that

2020 JINST 15 T01005

has higher core loss than some more advanced alloys, but this property can be compensated by increasing the core size. The use of iron is advantageous if cost is more important than mass and size. The experimental testing items included the output current ripple, output current bandwidth and the measured magnetic field and output current relationship at different frequencies. Long-term stability testing also provides important experimental data. Hence, the full load was measured for 8 hours, and the current change was observed. Figure 6 shows the iron core magnet loading test in the laboratory.

Figure 6. Iron core magnet loading.

Figure 7 and table 1 show the corrector power supply and specification with input voltage of 48 V and output current and voltage of ±10 A and ±40 V, respectively. The output current ripple needs to be less than ±0.1 mA peak-to-peak in 1–10 kHz. The long-term current stability needs to be within ±2 mA peak-to-peak. The current setting resolution is 20 bits. The current feedback resolution is 19 bits at full scale 10 A. The maximum resolution of 64 µA was reached. The switching frequency was increased to 145 kHz, which greatly optimised the bandwidth to 10 kHz.

Figure 7. Corrector magnet power supply.

Table 1. Corrector power supply specification.

	Corrector
Type	Bipolar, switched-mode
Input Voltage	48 V ± 10%
Maximum Current/voltage rating	±10 A/±40 V
Current control range	−10–10 Ampere
Current accuracy	Within ±1 mA
Current stability (0–30 min)	Within ±1 mA peak-to-peak
Current stability (0–8 h)	Within ±2 mA peak-to-peak
Current reproducibility	Within ±1 mA
Current ripple (frequency from 1 Hz to 10 kHz)	Within ±1 mA peak-to-peak
Current setting resolution	20 bits
Current feedback resolution	19 bits
Voltage feedback resolution	19 bits

4.1 MOSFET power switching waveforms

In electronics,[3] switching frequency refers to the rate at which an electronic switch[4] performs its function. Switching frequency is an important design and operating parameter in systems. It indicates the rate at which the DC voltage is switched on and off during pulse width modulation in a switching power supply. The switching frequency in an inverter or converter is the rate at which the switching device is turned on and off. Typical frequencies range from 20 kHz to 2 MHz. The increase in switching frequency can reduce the output filter inductor and capacitor. Simultaneously, the bandwidth of the corrector magnet power supply can be increased. For this prototype, the bandwidth can reach up to 10 kHz. Figure 8 shows the $S1$ & $S2$ MOSFET (IXFK180N15) gate signal and drain to source voltage waveforms (Ch1: V_{gs1}, Ch2: V_{ds1}, Ch3: V_{gs2}, Ch4: V_{ds2}) during a duty cycle. Figure 8 shows that the turned on of $S1$ transition is longer than $S2$ transition, and the output is in the positive current mode. Conversely, the turned on $S2$ is greater than $S1$ when the output is in the negative current mode. The main power switch supplies 145 kHz. A 20 ns delay was observed between the off and on gate signals. This delay time ensures that the MOSFET is completely turned off before the other MOSFET is turned on, thereby avoiding a shoot-through situation.

4.2 Output current ripple

Current ripple in electronics is the residual periodic variation of the DC current within a power supply, which is derived from an alternating current (AC) source. This ripple is due to the incomplete suppression of the alternating waveform after rectification. For this prototype, a rectifier inductor

[3]https://en.wikipedia.org/wiki/Electronics.
[4]https://en.wikipedia.org/wiki/Electronic_switch.

2020 JINST 15 T01005

Figure 8. MOSFET Power Switching Waveforms.

and capacitor are used to reduce the output current ripple. A 40 µH rectifier inductor was placed parallel to a 2.46 µF capacitor, whereas a 33 µF damping circuit capacitor was placed in series with a 10 Ω resistor. Figure 9 shows the measured output current ripple waveform for a full load of 10 A output current. The output current was measured using a dynamic signal analyser HP35670A, and the frequency of scan was 1–12.8 kHz. The maximum output current ripple was 12.75 µA at 10 kHz, and the required output current was satisfied within ±0.1 mA peak-to-peak power supply specification.

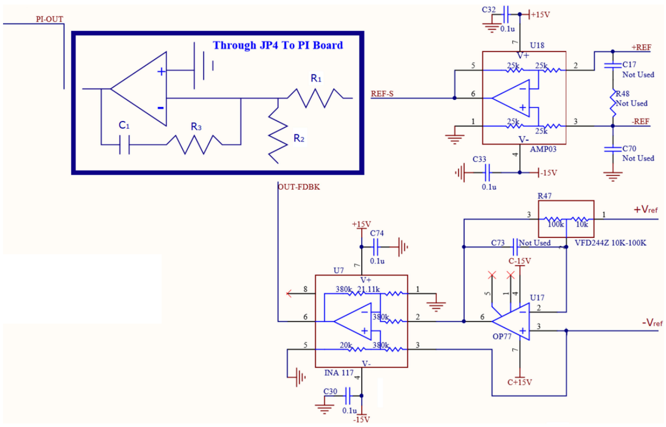

Figure 9. Output Current Ripple Waveform.

4.3 Long term stability

The parameter of electronic device is thermally dependent, and the temperature inside increases during the operation of the power supply. Therefore, the output current devices of control circuitry are unable to stabilise, and the output current remains unstable. Keeping the devices of control circuitry of power supply in a temperature controlled environment is straightforward and is the best way to achieve high output current stability. The long-term output current stability of corrector magnet power supply in (NSRRC) requires ±1,000 ppm (equal to 1 mA). The stability of the beam current depends on the constant output current for a long time. This prototype power supply must have high precision and constant output current during an 8 hours period. During this time, energy is supplied to the magnet load. The HP 34410 8.5 digital multi-meter and LEM IT 600-S Ultrastab DCCT were used for measurements. Figure 10 shows the output current of 10 A at full-load testing, and the output current is within ±0.2 mA peak-to-peak or within ±20 ppm.

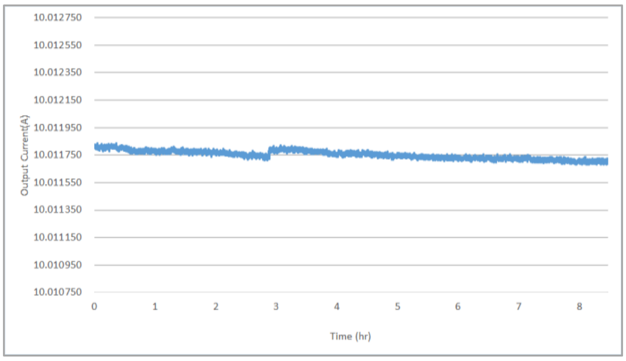

Figure 10. Output Current Long-Term Stability.

4.4 Bandwidth

The power bandwidth of an amplifier is sometimes considered the frequency range for which the rated power output of an amplifier can be maintained to at least half of the full-rated power. Current amplifiers often use the term full current bandwidth to indicate the highest frequency at which the achievable peak-to-peak output current swing is equal to the DC output current range.

In this study, the frequency response of the corrector power supply was measured using a dynamic signal analyser HP35670A in the frequency range of 10–51 kHz. The input DC voltage was 48 V. The reference signal was 100 mV sweep sine waveform to prototype. Figure 11 shows a corrector power supply bandwidth of −20 dB at 10 Hz with amplitude attenuation of −23.13 dB at 350 Hz. Figure 11 shows the prototype corrector power supply bandwidth of −20 dB at 10 Hz with amplitude attenuation of −23.05 dB at 11.2 kHz. The prototype increased the bandwidth from 350 Hz to 11.2 kHz (equivalent to 32 times), which greatly contributed to the performance optimisation of the accelerator. This power supply enabled the operation to proceed at a considerably high frequency region. The FOFB system can be operated at 10 kHz to increase the calculated number and improve beam current stability.

5 Conclusions

A novel high-frequency corrector power supply was developed for the TPS upgrade with high bandwidth, high stability of output current and low ripple. The test results indicated the operation of a corrector magnet power supply with a bandwidth of 11.05 kHz for a small signal of 1% of the

2020 JINST 15 T01005

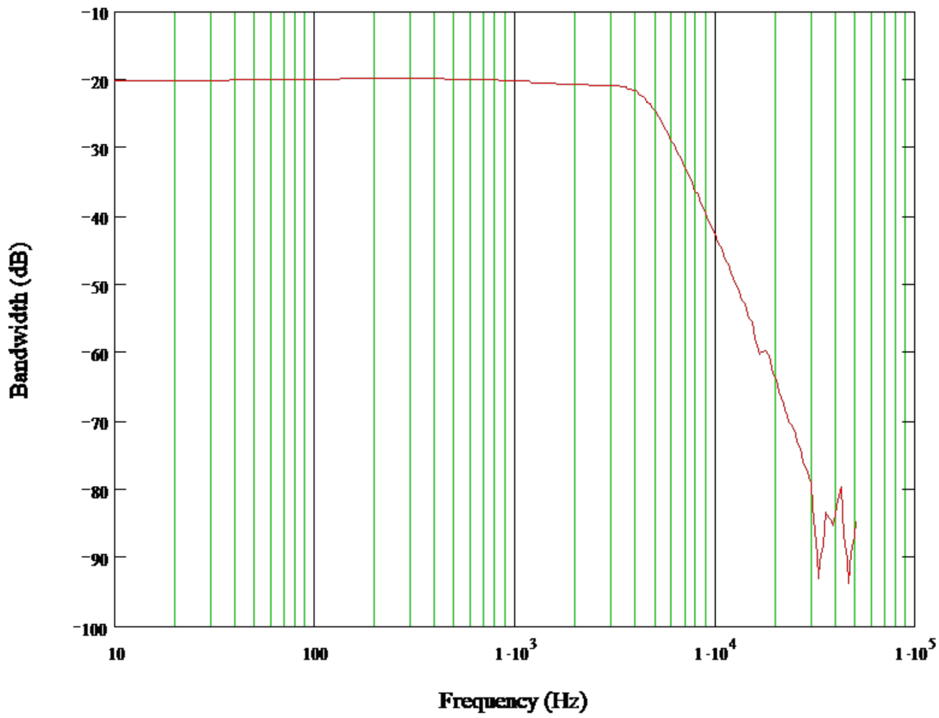

Figure 11. Previous Corrector Power Supply Bandwidth.

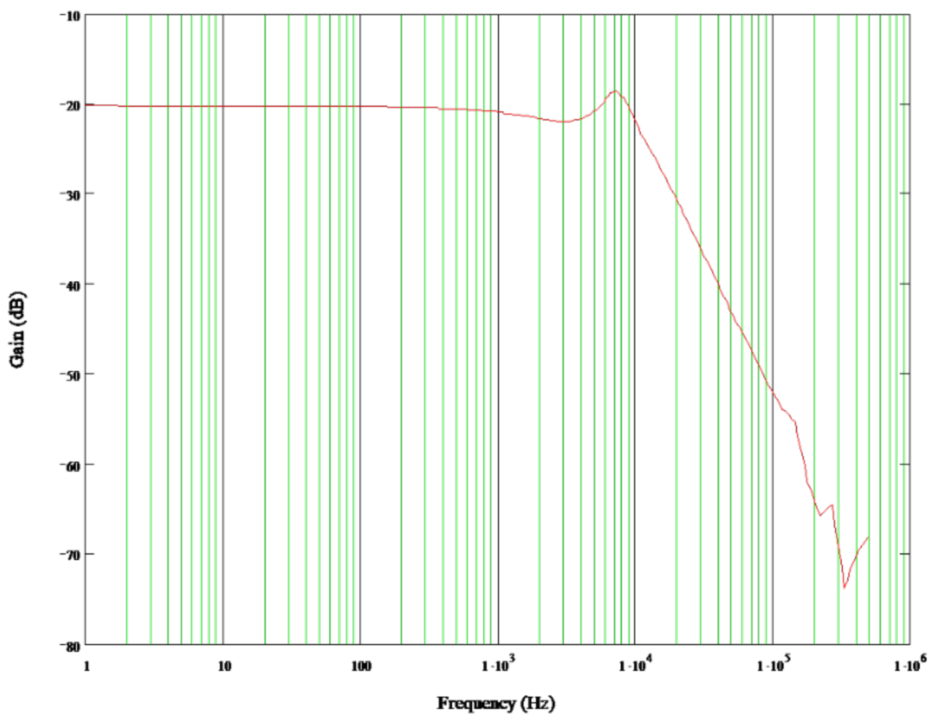

Figure 12. Prototype Corrector Power Supply Bandwidth.

full range. This is currently the highest bandwidth for the power supply in the accelerator field with a frequency response time of less than 100 µs. It can quickly adjust error correction value to beam current, which has a significant effect on the stability of beam current. The maximum output current ripple was 12.75 µA at 10 kHz, thereby satisfying the required output current of within ±0.1 mA peak-to-peak power supply specification. When the output current of 10 A was subjected to full-load testing for a long time (8 hours), the output current variation was 10 µA within ±0.2 mA peak-to-peak or within ±20 ppm.

Acknowledgments

This work was supported by the magnet group, which is a member of the National Synchrotron Radiation Research Center. The authors also gratefully acknowledge the helpful comments and suggestions of the reviewers, which improved the presentation.

References

[1] F. Trillaud, S. Prestemon, R. Schlueter and S. Marks, *Design of a Cryogenic Calorimeter for Synchrotron Light Source Beam-Based Heating*, *IEEE Trans. Appl. Supercond.* **19** (2009) 2321.

[2] Y.-S. Wong, J.-F. Chen, K.-B. Liu, C.-Y. Liu and B.-S. Wang, *Compensator Design for Corrector Magnet Power Supply of TPS Facility*, 2017 *JINST* **12** T10001.

[3] K.-B. Liu, Y.-D. Li, B.-S. Wang, K.-T. Hsu and J.C. Hsu, *TPS Corrector Magnet Power Converter*, in proceedings of the *1st International Particle Accelerator Conference (IPAC 2010)*, Kyoto, Japan, 23–28 May 2010, pp. 3269–3271 [*Conf. Proc.* **C 100523** (2010) WEPD073].

[4] K.-B. Liu and J.T. Sheu, *High Output Current Stability of Power Supply*, in proceedings of the *7th European Particle Accelerator Conference (EPAC 2000)*, Vienna, Austria, 26–30 June 2000, pp. 2214–2216.

[5] A. Napier, S. Gayadeen and S.R. Duncan, *Fast Orbit Beam Stabilisation for a Synchrotron*, in proceedings of the *2011 IEEE International Conference on Control Applications (CCA)*, Denver, CO, U.S.A., 28–30 September 2011, pp. 1094–1099 [https://doi.org/10.1109/CCA.2011.6044452].

[6] J. Wang and G. Sprau, *A High Bandwidth Bipolar Power Supply for the Fast Correctors in the APS Upgrade*, in proceedings of the *2nd North American Particle Accelerator Conference (NAPAC2016)*, Chicago, Illinois, U.S.A., 9–14 October 2016, pp. 96–98.

[7] Y.-S. Wong, J.-F. Chen, K.-B. Liu and Y.-P. Hsieh, *A Novel High Step-up DC-DC Converter with Coupled Inductor and Switched Clamp Capacitor Techniques for Photovoltaic Systems*, *Energies* **10** (2017) 378.

[8] B. Song and J. Wang, *Mathematical Modelling and Analysis of a Wide Bandwidth Bipolar Power Supply for the Fast Correctors in the APS Upgrade*, in proceedings of the *6th International Particle Accelerator Conference (IPAC 2015)*, Richmond, Virginia, U.S.A., 3–8 May 2015, pp. 3264–3266.

[9] P. Bellomo and A. de Lira, *SPEARS3 Intermediate DC Magnet Power Supplies*, in proceedings of the *3rd Asian Particle Accelerator Conference (APAC 2004)*, Gyeongiu, Korea, 22–26 March 2004, pp. 61–63.

[10] N. Tani, Y. Watanabe, H. Hotchi, T. Takayanagi, T. Togashi and K. Horino, *Optimization of the Pole Shape for Corrector Quadrupole Magnet in the J-PARC* 3*-GeV RCS*, *IEEE Trans. Appl. Supercond.* **26** (2016) 1.

[11] E.J. Prebys et al., *New Corrector System for the Fermilab Booster*, in proceedings of the *2007 IEEE Particle Accelerator Conference (PAC)*, Albuquerque, NM, U.S.A., 25–29 June 2007, pp. 467–469 [https://doi.org/10.1109/PAC.2007.4440247].

[12] D.J. Harding et al., *Design and Fabrication of a Multi-element Corrector Magnet for the Fermilab Booster Synchrotron*, in proceedings of *2007 IEEE Particle Accelerator Conference (PAC)*, Albuquerque, NM, U.S.A., 25–29 June 2007, pp. 452–454 [https://doi.org/10.1109/PAC.2007.4440242].

[13] M. Bickley, B.A. Bowling, D. Douglas, A. Hofler, J. Kewisch and G.A. Krafft, *Orbit Correction Implementation at CEBAF*, in proceedings of the *International Conference on Particle Accelerators*, Washington, D.C., U.S.A., 17–20 May 1993, pp. 1895–1897 [https://doi.org/10.1109/PAC.1993.309168].

[14] W.J. Corbett, M.J. Lee and V. Ziemann, *A Fast Model Calibration Procedure for Storage Rings*, in proceedings of the *International Conference on Particle Accelerators*, Washington, D.C., U.S.A., 17–20 May 1993, pp. 108–110 [https://doi.org/10.1109/PAC.1993.308999].